JOURNAL OF MAGNETIC RESONANCE **127,** 229–232 (1997)
ARTICLE NO. MN971205

COMMUNICATIONS

Fast Automatic Adjustment of On-Axis Shims for High-Resolution NMR

Jun Shen[1] and Douglas L. Rothman

Magnetic Resonance Center, Yale University School of Medicine, New Haven, Connecticut 06510

Received January 30, 1997; revised April 21, 1997

A one-dimensional approach for fast, robust, automatic adjustment of on-axis shims on high-resolution NMR spectrometers based on polynomial fitting of field inhomogeneity is described. Spherical harmonic and nonspherical harmonic terms of the field distribution of shim coils are precalibrated as polynomial coefficients by successively changing shim settings. This method greatly simplifies the shim precalibration and optimization procedures and is readily to be extended to three-dimensions to include off-axis shims.

The importance of shimming in NMR spectroscopy is well known. The practical approach to shimming in high-resolution NMR spectroscopy has been based on iterative procedures which are time-consuming due to the interactions between shim coils and existence of many local minima. With the advent of high-field spectrometers optimization of field homogeneity becomes more demanding since susceptibility effects increase with increasing B_0 field strength. Automatic shimming techniques based on chemical shift imaging (*1, 2*) or phase differences (*3–9*) have been well established for *in vivo* imaging and spectroscopy applications. The basic idea is to measure the spatial dependence of B_0 inhomogeneity using triple-axis gradients followed by shim adjustments based on the measured or calculated characteristics of the individual shim coils. With gradient accessories becoming more available to high-resolution spectrometers these automatic shimming methods can also benefit high-resolution NMR spectroscopy. Recently, van Zijl *et al.* (*10*) introduced a three-dimensional gradient-recalled echo imaging method to automatic shimming for high-resolution NMR spectrometers. This method and its one-dimensional version measure the true characteristics of shim coils and then solve for the optimal shim settings using a singular value decomposition algorithm. The three-dimensional method has been shown to perform the complete shimming process (acquisition and data processing) in 4.5 min and be able to adjust 28 shims with 3–4 iterations from zero shim currents to optimal field homogeneity on modern spectrometers equipped with a SGI workstation. In this Communication, we propose an alternative approach based on spherical harmonic field distribution of shim coils (*7–9*). Like its *in vivo* version, this approach simplifies the shim precalibration and optimization procedures, allowing its implementation on spectrometers equipped with older computers. Only the one-dimensional method is discussed here using a single-axis gradient probe. Where triple-axis gradient probes are available, tilted linear projections can be generated to adjust off-axis shims, avoiding 3D data acquisition and processing.

The 1D method described here was implemented on a BRUKER AM 500-MHz spectrometer. The system is equipped with the following shim coils: z, z^2, z^3, z^4, z^5 (on-axis), and x, y, $x^2 - y^2$, xy, xz, yz, x^3, y^3, xz^2, yz^2, zxy, $z(x^2 - y^2)$ (off-axis) and a z-axis gradient probe (5 mm). Shim calculations and adjustment were performed using a Pascal program run by the spectrometer computer (ASPECT 3000). Each iteration (acquisition, Fourier transform, shim calculation and adjustment) takes ca. one minute on the ASPECT 3000 computer. Three to four iterations are needed to achieve a full convergence of on-axis shims starting from zero shim current. For a standard setup starting from a default shim file, only 1–2 iterations are necessary. An acronym suitable for this method is ZIGZAG as deduced from zero *i*nhomogeneity *g*enerated using a *z a*xis *g*radient.

Figure 1 shows the gradient echo pulse sequence used for encoding B_0 inhomogeneity along the z axis. A selective pulse is applied to excite an on-resonance singlet. Deuterium lock should be on during the acquisition to avoid field drifting. The gradient strength used is 250 Hz/mm with a field of view (FOV) of 5 cm. The echo time employed is 10

[1] To whom correspondence should be addressed.

1090-7807/97 $25.00

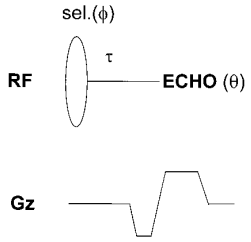

FIG. 1. Pulse sequence for 1D automatic shimming. The delay τ is set to zero and a nonzero value to obtain a phase difference map along the z direction. $\phi = x, -x$; $\theta = x, -x$. A nonselective pulse can be used if the spectrum is dominated by a major peak such as water.

ms with 128 complex points sampled to generate a spatial resolution of 0.4 mm/point. The phase difference between two profiles with $\tau = 0$ and $\tau <> 0$ (usually 10–50 ms) is automatically corrected (*7*) for 0°/360° phase transitions assuming phase difference between adjacent points do not exceed 60°, which corresponds to a maximum B_0 gradient of less than 43–8 Hz/mm. The phase difference divided by $\Delta\tau$ is proportional to the z component of B_0 inhomogeneity, which can be expanded into a polynomial series

$$B_0(z_j) = \sum_i a_i z_j^i, \qquad [1]$$

where z_j is the jth ordinate along z axis, and a_i is the ith-order polynomial coefficient.

Ideally, each shim coil should produce a B_0 field with a certain spherical harmonic spatial dependence, which can be precalibrated independent of the sample by measuring the change of the corresponding polynomial coefficient while successively changing its current. Then for an unknown inhomogeneous field, a polynomial regression can be performed to calculate the polynomial coefficients which are proportional to the corresponding on-axis shim current adjustments. In our case, the z, z^2, z^3, z^4, and z^5 shims are calculated by

$$\begin{bmatrix} \sum_j z_j^2 & \sum_j z_j^4 & \sum_j z_j^6 \\ \sum_j z_j^4 & \sum_j z_j^6 & \sum_j z_j^8 \\ \sum_j z_j^6 & \sum_j z_j^8 & \sum_j z_j^{10} \end{bmatrix} \begin{bmatrix} a_1 \\ a_3 \\ a_5 \end{bmatrix} = \begin{bmatrix} \sum_j z_j B_0(z_j) \\ \sum_j z_j^3 B_0(z_j) \\ \sum_j z_j^5 B_0(z_j) \end{bmatrix}$$

and

$$\begin{bmatrix} N & \sum_j z_j^2 & \sum_j z_j^4 \\ \sum_j z_j^2 & \sum_j z_j^4 & \sum_j z_j^6 \\ \sum_j z_j^4 & \sum_j z_j^6 & \sum_j z_j^8 \end{bmatrix} \begin{bmatrix} a_0 \\ a_2 \\ a_4 \end{bmatrix} = \begin{bmatrix} \sum_j B_0(z_j) \\ \sum_j z_j^2 B_0(z_j) \\ \sum_j z_j^4 B_0(z_j) \end{bmatrix}, \qquad [2]$$

where N is the total number of data points. Due to imperfect field centering of shim coils and imperfect spherical

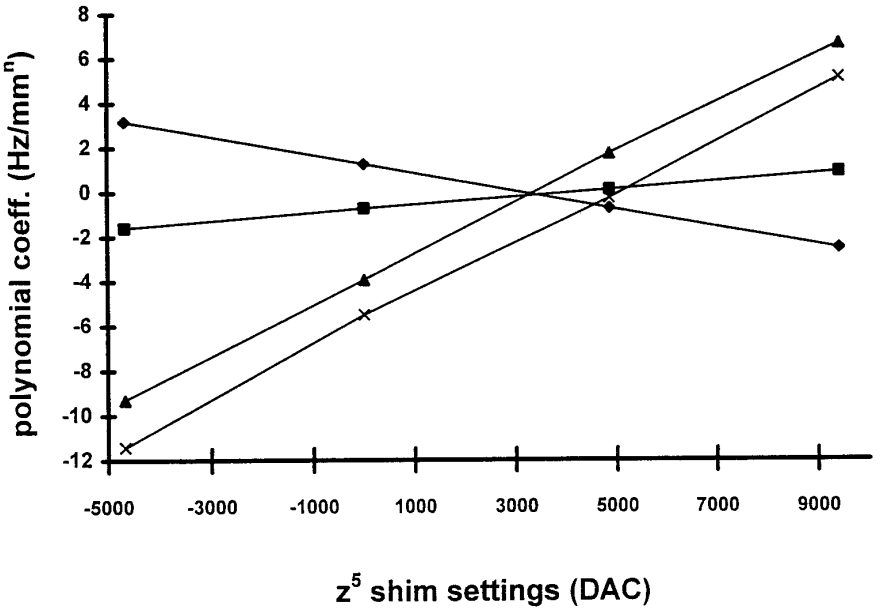

FIG. 2. Calibration of z^5 shim coils and its interactions with z, z^3, and z^4 shim coils. ♦, $a_5(z^5) \times 10^4$ Hz/mm^5; ■, $a_1(z^5)$ Hz/mm; ▲, $a_3(z^5) \times 10^3$ Hz/mm^3; ×, $a_4(z^5) \times 10^4$ Hz/mm^4. The slopes of the calibration curves obtained by linear regression are $k_{a5(z5)} = -4.044 \times 10^{-8}$ Hz/mm^5, $k_{a1(z5)} = 1.766 \times 10^{-4}$ Hz/mm, $k_{a3(z5)} = 1.136 \times 10^{-6}$ Hz/mm^3, $k_{a4(z5)} = 1.164 \times 10^{-7}$ Hz/mm^4.

harmonic field distribution there are interactions between shim coils. These interactions make conventional shimming a tedious process, especially when the center of shim set and the center of the sample are not coincident. Using the z-axis field mapping proposed here, shim interactions can be easily calibrated independent of sample positioning in terms of polynomial coefficients and subtracted from the coefficients of affected shims before shim adjustments.

Figure 2 shows the example of calibration of the z^5 shim coil around $a_5 = 0$ as well as its interactions with the z, z^3, and z^4 shims. The z^5 shim current was set to different values without changing other shims. The field maps measured were fitted by a polynomial series (Eq. [2]) to obtain the corresponding polynomial coefficients due to changes in the z^5 shim settings. No significant interaction with the z^2 shim was found for the z^5 shim. All correlations were found to be linear. The adjustment of the z^5 shims for an unknown field inhomogeneity can be made using a_5 calculated from Eq. [2] and the linear relationship between the changes in z^5 shim settings and the changes in a_5 as shown in Fig. 2. For lower order shims, the contributions from higher order shims need to be subtracted from the corresponding polynomial coefficients calculated using Eq. [2] before conversion to changes in their shim settings:

$$\Delta I_i = (a_i - \sum_j a_j k_{ji}/k_j)/k_i \ (j > i), \qquad [3]$$

where ΔI_i is the adjustment of the current of the ith-order shim, $k_i = (\partial a_i/\partial I_i)_{n\neq i}$, $k_j = (\partial a_j/\partial I_j)_{n\neq j}$, $k_{ji} = (\partial a_i/\partial I_j)_{n\neq j}$.

To demonstrate the effectiveness of this method, the field inhomogeneity of a sample of 50% H_2O/50% D_2O was measured after the high-order shims were deliberately misadjusted for correction by automatic shimming. The result is shown in Fig. 3a (solid line). The dotted-dashed line is the fifth-order polynomial fit. The B_0 field after one round of automatic shimming is shown in Fig. 3b (solid line). The polynomial fit (dotted-dashed line) is for the next iteration. Figure 3c shows the residual field inhomogeneity after a total of two iterations. Two scans were taken for each echo. The sample was not spun, and off-axis shims were not adjusted.

Figure 4 shows the spectral region upfield from water of a sample of 1.5 mM sucrose in 90% D_2O/10% H_2O shimmed using three iterations starting from zero shim currents for on-axis shims. The sample tube was spun at 20 Hz. No attempt was made to remove paramagnetic species such as O_2 and trace heavy metal impurities. The off-axis shims were crudely adjusted by hand shimming before recording the spectrum. This was to minimize spinning side bands. Excellent resolution was achieved within a short amount of time. We have also performed automatic shimming on a shimming

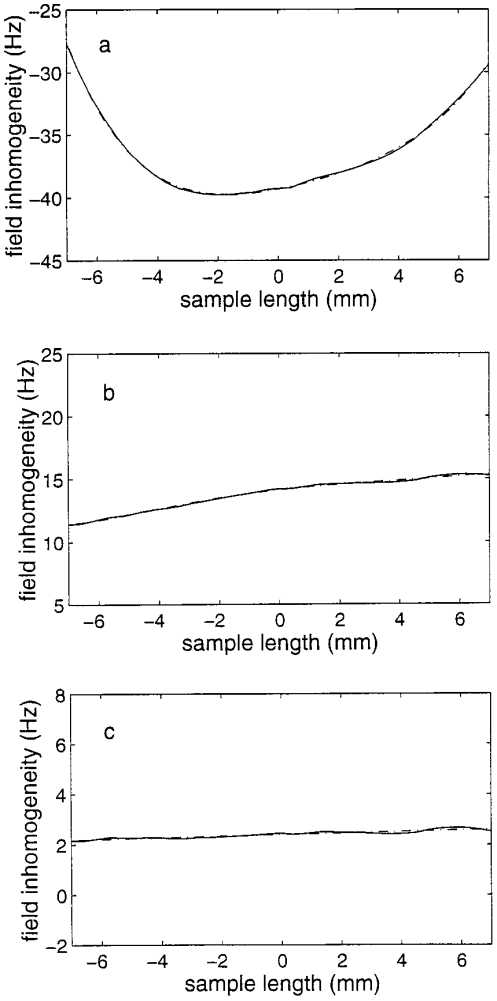

FIG. 3. (a) Field inhomogeneity (solid line) of a 2.8-cm-length 50% H_2O/50% D_2O sample measured and the corresponding fifth-order polynomial fit (dotted-dashed line) before automatic shim corrections. Part of the sample, 1.4 cm, was used for shimming calculations. (b) Field inhomogeneity (solid line) after one iteration of ZIGZAG and the fifth-order polynomial fit (dotted-dashed line) for the next iteration. (c) Field inhomogeneity after the second iteration. $\tau = 20$ ms was used.

standard ODCB provided by Bruker by selectively exciting the TMS singlet. A half-height width of 0.1 Hz was obtained after four iterations (data not shown).

With enough S/N, any shimming methods based on field mapping ideally should give a close to perfect adjustment of on-axis shims using a single iteration if all interactions among shims are taken into account. In reality, gradient nonlinearity and B_0 inhomogeneity make $r_j <> j$*FOV/N, resulting in inaccurate spatial encoding. Errors in shim calibrations also contribute to inaccurate shim adjustments during a single iteration. Therefore, 3–4 iterations are generally needed to achieve a full convergence if the starting shims are far off. Our method is no exception.

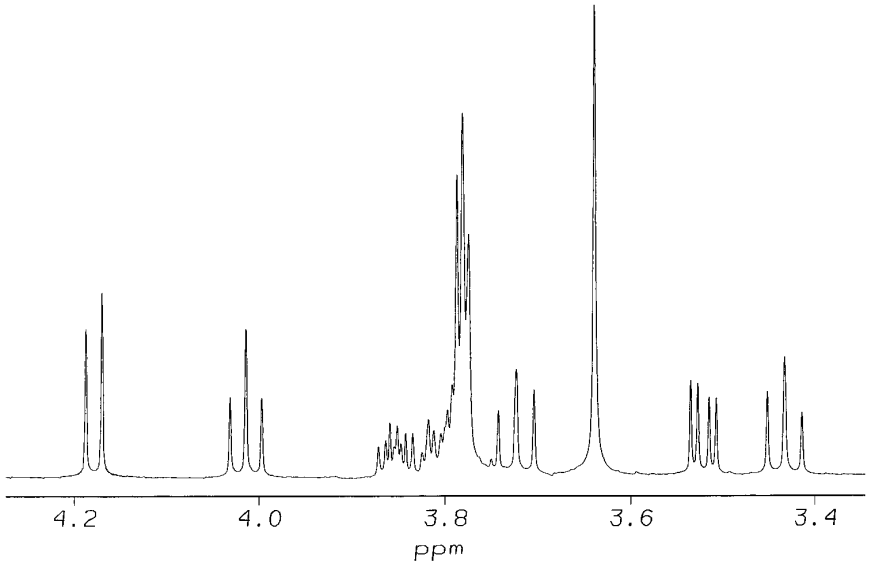

FIG. 4. ^{1}H spectral region upfield from water of a sample containing 1.5 m*M* sucrose in 90% D_2O/10% H_2O taken after three iterations of our 1D automatic shimming method while spinning. No window functions were used.

In conclusion, we have demonstrated that it is possible to automatically obtain optimal adjustment of on-axis shims based on the imperfect spherical harmonic field distribution of shim coils. The same principles should apply to off-axis shims. This should greatly reduce the time needed for precalibration and optimization of shims, making automatic shimming available to any spectrometers equipped with gradient accessories.

ACKNOWLEDGMENTS

We thank Terry Nixon for improvements to and maintenance of the spectrometer, and Professor Robert G. Shulman for advice and support. This work was supported by NIH First Award R29 NS32126-02 to D. L. Rothman, and NIH Grants R01 EY10856-02 and R01 DK27121-46 to R. G. Shulman.

REFERENCES

1. J. Tropp, K. A. Derby, C. Hawrysko, S. Sugiura, and H. Yamagata, *J. Magn. Reson.* **85,** 244 (1989).
2. F. A. Jaffer, H. Wen, R. S. Balaban, and S. D. Wolff, *Magn. Reson. Med.* **36,** 375 (1996).
3. M. G. Prammer, J. C. Haselgrove, M. Shinnar, and J. S. Leigh, *J. Magn. Reson.* **77,** 40 (1988).
4. E. Schneider and G. Glover, *Magn. Reson. Med.* **18,** 335 (1991).
5. P. Webb and A. Macovsky, *Magn. Reson. Med.* **20,** 113 (1991).
6. A. M. Blamire, D. L. Rothman, and T. Nixon, *Magn. Reson. Med.* **36,** 159 (1996).
7. R. Gruetter and C. Boesch, *J. Magn. Reson.* **96,** 323 (1992).
8. R. Gruetter, *Magn. Reson. Med.* **29,** 804 (1993).
9. J. Shen, R. E. Rycyna, and D. L. Rothman, *Magn. Reson. Med.,* in press.
10. P. C. M. van Zijl, S. Sukumar, M. O'Neil Johnson, P. Webb, and R. E. Hurd, *J. Magn. Reson. A* **111,** 203 (1994).